

Task-Driven In-Hand Manipulation of Unknown Objects with Tactile Sensing

Chaoyi Pan*, Marion Lepert*, Shenli Yuan, Rika Antonova, Jeannette Bohg

Abstract—Manipulation of objects in-hand without an object model is a foundational skill for many tasks in unstructured environments. In many cases, vision-only approaches may not be feasible; for example, due to occlusion in cluttered spaces. In this paper, we introduce a method to reorient unknown objects by incrementally building a probabilistic estimate of the object shape and pose during task-driven manipulation. Our method leverages Bayesian optimization to strategically trade-off exploration of the global object shape with efficient task completion. We demonstrate our approach on a Tactile-Enabled Roller Grasper, a gripper that rolls objects in hand while continuously collecting tactile data. We evaluate our method in simulation on a set of randomly generated objects and find that our method reliably reorients objects while significantly reducing the exploration time needed to do so. On the Roller Grasper hardware, we show successful qualitative reconstruction of the object model. In summary, this work (1) presents a system capable of simultaneously learning unknown 3D object shape and pose using tactile sensing; and (2) demonstrates that task-driven exploration results in more efficient object manipulation than the common paradigm of complete object exploration before task-completion.

I. INTRODUCTION

This work studies how robots can reorient objects in-hand with limited prior knowledge about object shape. Manipulating objects of unknown shapes is a foundational skill that robots need to perform tasks in unstructured environments. For example, to be useful in a kitchen, a robot must be able to pick up and manipulate a breadth of objects such as fruits and vegetables whose shapes cannot be known beforehand. While vision is a powerful modality to gain information about novel objects, there are many scenarios where vision cannot be used, such as in cluttered spaces with high occlusion and during manipulation of small objects where it is likely that the gripper will occlude the object. Therefore, robots must learn to manipulate objects with sensors other than vision. Tactile sensing is an attractive modality because it provides high-resolution local information about contact between the object and gripper, which is complementary to global vision information.

Object reorientation with tactile sensing is challenging because tactile data gives information about the object shape for only a small contact patch area, so the object’s global shape needs to be pieced together from limited local information. In addition, the object may only have a limited set of features

*Authors contributed equally and names are in random order. Chaoyi Pan is with Tsinghua University. Marion Lepert, Shenli Yuan, Rika Antonova, and Jeannette Bohg are with Stanford University [lepertm, shenliy, rika.antonova, bohg]@stanford.edu. Toyota Research Institute provided funds to support this work. We are grateful to Shaoxiong Wang for help with the Roller Grasper. Rika Antonova is supported by the National Science Foundation grant No.2030859 to the Computing Research Association for the CIFellows Project.



Fig. 1: Roller Grasper reorienting a small object.

that the tactile sensor can detect to distinguish between different locations on the object. Moreover, the object may shift slightly between the times when the tactile readings are obtained, which increases uncertainty regarding the location of these readings.

We propose a method to reorient unknown objects by incrementally building a probabilistic estimate of the object shape during manipulation. Our method leverages Bayesian optimization to strategically trade off exploration of the global object shape with efficient task completion. We demonstrate our approach on a Roller Grasper that rolls objects in hand and continuously collects tactile data, as shown in Fig. 1.

We consider the class of tasks where the robot cannot rely on vision and instead has to use tactile sensing to feel the object’s shape and localize it in space. To ensure that the robot does not have access to the object shape before completing the task, we avoid using an image or point cloud to specify the target orientation of the object to be manipulated. Instead, we formulate our task as an insertion task. The robot is given an image of a hole, and the robot must determine how to reorient an object to fit into that hole. The shape of the hole provides minimal, but task-relevant, information about the 3D-shape of the object, ensuring that our assumption that the robot is working with an unseen object holds. We evaluate our method in simulation on a set of randomly generated objects and find that our method reliably completes the insertion task while significantly reducing the exploration time needed to do so. We also show qualitative results on real robot hardware.

To summarize, our main contributions are:

- A system to reorient unknown objects that does not rely on vision and instead leverages tactile sensing.
- An in-hand 3D simultaneous shape reconstruction and localization method to estimate an object’s shape and pose that is task driven.

II. RELATED WORK

A. In-hand manipulation

In-hand manipulation has been studied extensively [1]–[8]. Many approaches require object pose which can be obtained with a marker tag [4], [5] or a 6D object pose estimator [6]. Alternatively, deep learning methods can obtain an end-to-end policy that doesn't require pose estimation. For example, [1] learns a controller to reorient a Rubik's cube and [8] presents a controller that can reorient many distinct objects, but both rely on vision and complex multi-fingered grippers. In contrast, [2] demonstrates how simpler hardware (parallel-jaw grippers) can use extrinsic dexterity to re-orient objects in-hand. Their approach is limited to simple cuboids and requires a 6D object pose estimator. [7] shows how a compliant gripper can robustly reorient objects in-hand using handcrafted open-loop primitives that don't require object pose or shape estimation.

B. Tactile Sensing for shape reconstruction and localization

Reconstructing object shape from vision and tactile data is a common research objective [9]–[11]. These works typically rely heavily on vision and tend to use tactile data simply to detect contact. However, many scenarios with heavy occlusion preclude good vision data, leading to a growing interest in reconstructing and/or localizing objects with just tactile data.

Low resolution tactile sensors [12]–[14] are typically used to obtain binary contact information. The development of vision-based high resolution tactile sensors, such as the GelSight [15], has greatly increased our ability to reconstruct and localize objects without vision. The GelSight outputs an RGB image of the tactile imprint, and photometric stereo is used to convert this image to a depth image. Others learn this mapping from data [16], or choose instead to learn a binary segmentation mask [17] to reduce noise. [15] showed one of the first uses of the GelSight for small object localization, further improved in [16], [18]. However, they require building a complete tactile map of the object before using it for localization.

Most works assume each tactile imprint is collected by making and breaking contact with the object. This introduces uncertainty in the relative position of tactile imprints. Instead, [14] maintains constant contact with the object to reduce robot movement and obtain higher fidelity data. However, they use a low resolution sensor and only consider a bowl shaped object fixed in space. [19] slide along a freely moving cable with a GelSight to estimate the cable's pose, but their method is specific to cables. By rolling objects in-hand, we also continuously collect tactile data, but do so for a more general set of freely-moving objects.

Most of these works narrow their scope either by reconstructing the shape of an unknown object with a known fixed pose, or by localizing an object with known shape and unknown pose. Recently, [20] proposed removing these limitations by simultaneously doing shape reconstruction and localization from tactile data. However, they only show results for pushing planar objects.

Gaussian process implicit surfaces (GPIS) are commonly used to build a probabilistic estimate of an object's shape [21]. [14], [22] use the variance of the GPIS to guide the exploration towards regions with highest uncertainty. However, the goal of these approaches is to reconstruct the object shape as accurately as possible. In contrast, we focus on exploration that prioritizes regions of the object that are likely to aid in solving a task, making our exploration more efficient at solving real robotic tasks. [23] also prioritizes exploring regions that help solve a task, but their task is limited to grasping an object.

C. Insertion Task

A lot of previous work on the peg insertion task is object-geometry specific [24]–[26]. For example, [27] assumes cylindrical peg shape; [28] uses vision and tactile data to enable insertion of complex shapes but assumes known peg geometry; [29] learns from forces measured during human demonstration, but requires successful demonstration of the specific peg shape. In contrast, our work assumes no prior knowledge of the peg shape, and instead learns an explicit peg object model. There is some prior work that aims to be robust to different peg geometries, such as [30], but it does not manipulate the peg in-hand.

D. Roller Grasper

In this work, we use the Tactile-Enabled Roller Grasper hardware from [31]. This gripper has 7 degrees of freedom, shown in Fig. 4, and each roller is equipped with a custom GelSight sensor [32]. The sensor's camera is inside the roller, fixed to the stator such that it points towards the grasping point, while the elastomer covers the rotating roller.

Because the Roller Grasper rolls objects in-hand, it can continuously collect tactile information of an object's surface. This continuity reduces uncertainty in relative position between tactile imprints, simplifying reconstruction of object shape compared to linkage-based grippers that capture discontinuous data.

Several works have studied the Roller Grasper. [4] proposed a velocity controller and an imitation learning controller to reorient objects. [31] built a closed loop controller that keeps an object centered in the Roller Grasper during manipulation using contact patch data from the tactile sensor. We build on these works by using the velocity controller to determine the roller action to produce a desired object angular velocity. However, we don't assume a known object model or use marker tags, and instead simultaneously reconstruct and localize the object in a task-driven manner.

III. APPROACH

We propose a method that leverages tactile sensing to reorient objects of unknown shapes in order to complete a task. We focus on settings with high occlusion where the robot cannot see the object it is manipulating, and must instead rely on its sense of touch and proprioception. We evaluate our method on an insertion task where the robot

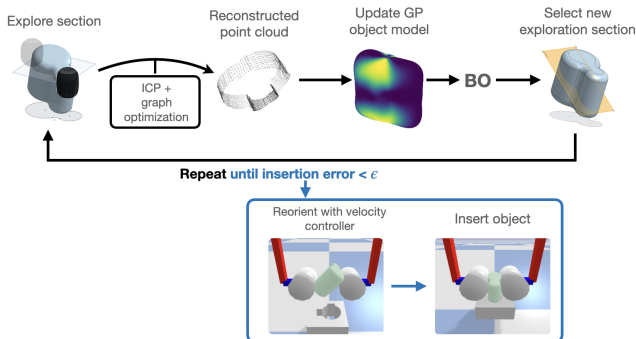


Fig. 2: A high-level overview of our method.

must reorient an object with a set of small and easily occluded features to fit into a hole. Our approach consists of three parts: shape estimation, task-guided exploration and in-hand reorientation. The shape estimation and task guided exploration are performed iteratively before the final in-hand reorientation.

- **Shape estimation:** The robot collects proprioception and tactile data as it rolls the object in-hand. We use the Iterative Closest Point (ICP) method [33] and graph optimization [34] to locally align the tactile data and estimate the global shape of the object along the touched contours. We fit a Gaussian process to this data to estimate the whole shape of the object.
- **Task guided exploration:** We decompose the insertion task into a form that allows us to leverage Bayesian optimization [35], [36] to guide the exploration of the object shape to efficiently complete the insertion task, reducing unnecessary exploration that is unlikely to aid in the completion of the task.
- **In-hand reorientation:** Once our exploration algorithm has high-confidence that it has found an orientation of the object that will fit in the hole, we localize the estimated object model using tactile data and use a velocity controller to reorient the object into the hole.

We focus on the insertion task to evaluate our approach because it avoids the dilemma of inadvertently giving object shape information to the robot through the target goal state. Formulating our task as an insertion task circumvents this issue because it gives the robot minimal prior object shape information, while still providing it with a clear goal to evaluate the core contribution of our method — task-driven in-hand manipulation with tactile sensing.

Assumptions: Because the Roller Grasper is physically incapable of reorienting objects with large aspect ratios without re-grasping, and because re-grasping is beyond the scope of this paper, we assume that the object to be manipulated has an aspect ratio close to 1. To enable the Roller Grasper to accurately reconstruct and localize objects, we also assume that our object has small features that can be detected by the tactile sensor which enable finding corresponding points on the object surface. We assume that an approximate initial placement of the object is known to allow us to easily grasp the object, since we focus on in-hand manipulation rather

than details of grasping. Since the Roller Grasper is position controlled, we assume we know the approximate width of the object to set the target distance between the rollers. This could be overcome by using a force sensor at each roller that would allow the grasper to regulate a desired grasping force.

A. Local shape estimation from tactile images

To estimate object shape, the Roller Grasper rolls the object in-hand and gathers joint position, $X \in \mathbb{R}^7$, and tactile RGB data, $I \in \mathbb{R}^{W \times H \times 3}$, at each time step. We convert a tactile RGB image to a depth map using a photometric stereo algorithm [32]. In simulation, we directly obtain the height map by placing a depth camera at the rollers.

We approximate the shape of the object by using the joint position data to estimate the transformation between the depth maps. Because the object occasionally slips on the roller surface, these estimates are noisy. We use ICP between local pairs of depth maps to reduce this noise and improve the fidelity of the reconstruction. Fig. 3 shows the benefits of using ICP to reconstruct small features on a real object.



Fig. 3: Left: Object to be manipulated, Middle: shape reconstruction without ICP, Right: shape reconstruction with ICP

Additionally, once the object has rotated at least 180 degrees, the rollers encounter regions of the object that have already been scanned by the other roller, as shown in Fig. 4. When we detect this loop closure, we use graph optimization [34] to align the two sets of point clouds.

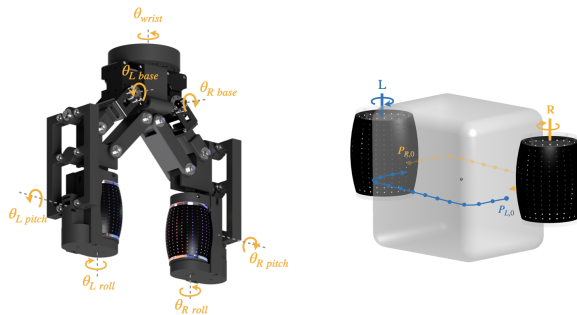


Fig. 4: Left: Degrees of freedom of the Roller Grasper. Right: After the object rotates 180°, we use graph optimization to close the loop between the data collected by the left roller (blue) and the right roller (yellow).

B. Global shape representation with Gaussian processes

Because the proprioception and tactile data collected by the Roller Grasper only give us partial information about the object shape, we use a Gaussian process (GP) to build a probabilistic estimate of the overall shape. We parameterize the surface of the object by spherical coordinates θ, ϕ, r . We use a GP to model the function $f(\theta, \phi) = r$ that represents the distance from the center of the object to its surface along

a ray parameterized by θ, ϕ . This GP model lets us predict the mean $f(\mathbf{x}_*)$ and variance $\mathbb{V}[f(\mathbf{x}_*)]$ of the distance to the object’s surface along any ‘query’ ray $\mathbf{x}_* := (\theta_*, \phi_*)$.

Formally, $\mathcal{GP}(m(\cdot), k(\cdot, \cdot))$ is a model defined by a prior mean function $m(\cdot)$ and kernel function $k(\cdot, \cdot)$. The prior $m(\cdot)$ is usually taken as zero. The kernel encodes similarity between inputs: a large $k(\mathbf{x}_i, \mathbf{x}_j)$ implies that observing the value $r_i = f(\mathbf{x}_i)$ for input \mathbf{x}_i would have a large influence on our estimate for $f(\mathbf{x}_j)$ for input \mathbf{x}_j . We can compute the posterior mean and variance using:

$$\bar{f}_* := \bar{f}(\mathbf{x}_*) := \mathbf{k}_*^T (K + \sigma_n^2 I)^{-1} \mathbf{r}, \quad (1)$$

$$\mathbb{V}[f_*] := \mathbb{V}[f(\mathbf{x}_*)] := k(x_*, x_*) - \mathbf{k}_*^T (K + \sigma_n^2 I)^{-1} \mathbf{k}_* \quad (2)$$

We obtain $\mathbf{r}, K, \mathbf{k}_*$ from the N points of the object’s point cloud $\{\mathbf{x}_i := (\theta_i, \phi_i), r_i\}_{i=1..N}$ constructed so far. $\mathbf{r} \in \mathbb{R}^N$ is a vector with distances from the object’s center to its surface (with entries $r_{i,i=1..N}$). $K \in \mathbb{R}^{N \times N}$ is a matrix with entries $k(\mathbf{x}_i, \mathbf{x}_j)_{i,j=1..N}$; $\mathbf{k}_* \in \mathbb{R}^N$ is a vector with entries $k(\mathbf{x}_*, \mathbf{x}_i)$. We use the Squared Exponential kernel function. We use GP marginal likelihood to estimate the kernel hyperparameters and the noise parameter σ_n automatically. See [37] for further details. Fig. 8 shows an example of incrementally building an object’s shape estimate with a GP.

C. Task Oriented Exploration

We use Bayesian optimization (BO) to guide our exploration of the object shape in order to efficiently identify regions of the object that are important for completing the insertion task. We construct a task oriented *acquisition* function for BO that selects the next target orientation of the object during in-hand manipulation. The aim is to select targets to reduce the uncertainty over the object shape globally, but focus on the promising regions and avoid over-exploring parts of the object unlikely to be useful for successful insertion. In contrast to related work that focuses on uniformly minimizing uncertainty for overall shape reconstruction, we use the task objective to achieve targeted exploration. Below we describe how we construct the task oriented acquisition function for BO.

We parameterize the object orientations relative to the target hole with angles α, β, γ , as shown in Fig. 5. For each orientation, we discretize the object into horizontal cross sections parameterized by l (and each cross section has a certain non-zero width). Our goal is to select the next object orientation and cross section to explore to help find an object orientation that will fit in the hole.

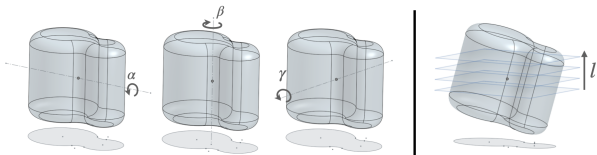


Fig. 5: Left: Object orientations relative to the target hole parameterized by angles α, β, γ . Right: Horizontal cross sections (placed along the vertical axis of the hole) that need to be analyzed for a given object orientation.

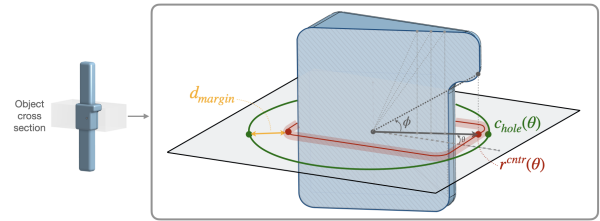


Fig. 6: For a given cross section of the object, this figure shows how the points on the object are projected onto a plane. We compare this projected contour to the contour of the hole to evaluate the fit of the object.

For calculating the optimal insertion orientation and determining which section to explore next, our pipeline starts by evaluating the margin distribution between the hole and the object in its current orientation α, β, γ at cross-section l .

We start with a probabilistic estimate of the object model in its current orientation. This model is a Gaussian process (GP) described in Section III-B above, which allows us to obtain estimates along any ray θ, ϕ for distance to object surface $R(\theta, \phi) \sim \mathcal{N}(\bar{f}, \mathbb{V}[f])$ in spherical coordinate system.

We begin by defining all the random variables we consider, their distributions, and the necessary discretization variables. θ_m with $m=1..M$ are equally spaced in the range $[-\pi, \pi]$; ϕ_n with $n=1..N$ are equally spaced in the range of the currently selected section l . By querying the GP at each angle pair (θ_m, ϕ_n) , we get a Gaussian distribution:

$$R_{m,n} \sim \mathcal{N}(\bar{f}(\theta_m, \phi_n), \mathbb{V}(f(\theta_m, \phi_n))) \quad (3)$$

Next, the object section is projected to the $x-y$ plane of the hole to calculate the ability of the object to fit through the hole in the selected orientation: $R_{m,n}^{\text{proj}} = R_{m,n} \cos(\phi_n)$. Note that for a given θ angle on the $x-y$ plane, the most protruding part of the object section will limit its ability to fit through the hole. Therefore, we are interested in taking the maximum of $R_{m,n}^{\text{proj}}$ over all ϕ_n for a given θ_m . We define the planar contour distribution as the distribution of the random variable $R_m^{\text{cntr}} := \max_n R_{m,n}^{\text{proj}}$. This distribution describes the object contour at angle θ_m in the plane of the hole (the $x-y$ plane).

Our goal is to produce a score for the current object orientation and section. Conceptually, this score should correspond to how likely this object section is to collide with the hole, which is dominated by the part of the object that is most likely to overlap with the edge of the hole (or is closest to the edge of the hole). Thus, for the current orientation, we want to compute the distribution that describes the maximum overlap (equivalently, the minimum margin between the object and the hole). For this, we first obtain a distribution D_m at each θ_m as: $D_m = c_m^{\text{hole}} - R_m^{\text{cntr}}$, where c_m^{hole} is a known scalar describing the hole radius at angle θ_m .

Now, we can define our score $S = \min_m D_m$ over all possible θ_m for the current orientation and section. We use this score to select the next orientation/section of the object to evaluate (i.e. the next desired object orientation to reach). Intuitively, we trade off between selecting an orientation that is most likely to position the object to fit through the hole

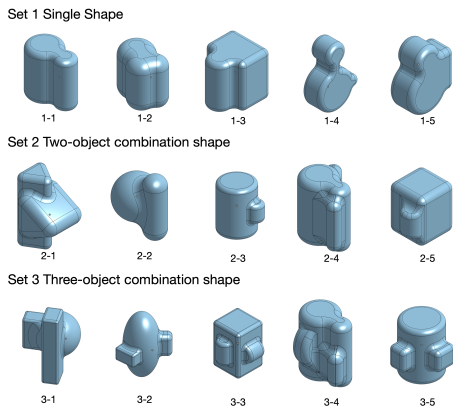


Fig. 7: The object set used for evaluation.

according to the current model (exploitation), and the orientation with the most uncertainty about its fit (exploration). We can use the mean and standard deviation of S to construct the following acquisition function, based on the upper confidence bound (UCB) function [38]:

$$UCB(\alpha, \beta, \gamma) = \mu_S(\alpha, \beta, \gamma) + \lambda \sigma_S(\alpha, \beta, \gamma), \quad (4)$$

where λ is a hyperparameter that controls the preference between exploitation and exploration. To select the next orientation, we maximize Equation 4 to obtain $\alpha^*, \beta^*, \gamma^*$.

Next, we choose the horizontal section of the object in the selected orientation $(\alpha^*, \beta^*, \gamma^*)$. Here, we trade off between selecting the horizontal section that is most likely to overlap the hole (exploitation) and the horizontal section with the most uncertainty (exploration). This ensures that we tend to examine the ‘worst’ sections of our ‘best’ orientations. This is motivated by the need to examine the sections in the ‘best’ orientation that are most likely to collide with the hole and cause task failure. If such ‘worst’ sections still fit, the entire object in this orientation is likely to fit into the hole. Formally, we select the parameter l^* (which defines the placement of the section to consider on the vertical axis) by maximizing the following function:

$$UCB_{\alpha^*, \beta^*, \gamma^*}(l) = -\mu_S(l) + \lambda \sigma_S(\alpha^*, \beta^*, \gamma^*)(l). \quad (5)$$

D. In-hand reorientation

We use the velocity controller from [4] to determine the rollers’ pitch angles $\theta_{L, \text{pitch}}, \theta_{R, \text{pitch}}$ and rollers’ angular velocities $\omega_{L, \text{roll}}, \omega_{R, \text{roll}}$ that are necessary to achieve the desired angular velocity of the object. The controller assumes that the object is a sphere, but we find that by adding compliance to the opening of the Roller Grasper, we can reorient a broader set of object shapes. However, due to the kinematics of the Roller Grasper, it is physically impossible to manipulate objects with a large aspect ratio, so we limit ourselves to objects with aspect ratios close to 1.

Due to torsional friction between the rollers and the object, when the roller grasper changes its pitch angle, the object may inadvertently rotate with the roller. This rotation is undesirable because it is hard to control the effects of

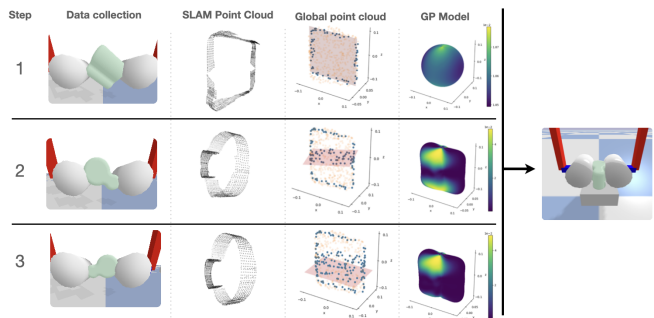


Fig. 8: A demonstration of the reorientation procedure. Each row corresponds to one exploration step. In the first column, the Roller Grasper picks up the object, rolls it in hand and captures tactile data from the Gelsight. In the second column, tactile SLAM merges the tactile image using ICP and graph optimization to get the section point cloud. The third column shows the down-sampled point cloud’s relative position to the whole object. The fourth column shows the probabilistic object model described by the GP. Our algorithm stops when the estimated insertion error is less than 3 mm.

torsional friction, and it prevents changing roller orientation relative to the object. To mitigate this, we lightly press the object against an external surface when changing the pitch angle of the rollers to prevent object rotation.

IV. EXPERIMENTAL EVALUATION

To experimentally test our method, we present quantitative evaluation of its effectiveness in simulation, and qualitative demonstration of its ability to reconstruct unknown object shape on the Roller Grasper hardware.

A. Simulated task oriented exploration

To evaluate our BO-based task guided exploration strategy, we measure the insertion task success rate and number of exploration steps required using 15 objects and 72 initial grasping points per object. An exploration step consists of a complete rotation of the object along a selected cross section.

Simulation environment. The simulation environment is built in PyBullet [39]. First, an object is instantiated in-hand with a random orientation sampled from a uniform distribution. Next the rollers roll the object in-hand to conduct tactile SLAM. When a closed loop is detected, the roller stops and proceeds to the next section determined by the selected algorithm. The exploration process stops when the insertion error is less than 3mm. To approximate real hardware, we add zero-mean Gaussian noise with $\sigma = 2\text{mm}$ (unless otherwise stated) to the reconstructed model.

Object set. Fig. 7 shows 15 different objects we used for evaluation, generated by randomly combining either one, two, or three randomly-transformed basic 3D shapes. The target hole shape is generated by projecting the object onto a plane, such that each object has only one feasible insertion orientation. Maximum object width is 5 centimeters.

Methods we compare.

- 1) Our method that uses Bayesian optimization to trade off between exploration and task completion, with λ tuned over a hold-out set of objects ($\lambda = 500$).
- 2) Random: selects sections for exploration from a uniform random distribution

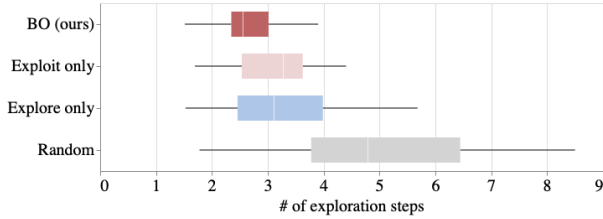


Fig. 9: Number of exploration steps required for successful object insertion using different algorithms in simulation. The boxplot indicates the 25th percentile, median, and 75th percentile over the 15 objects tested.

- 3) **Exploit-only:** without considering uncertainty, selects the object orientation that is most likely to allow insertion and checks the section in that orientation that is most likely to cause a failure. This is equivalent to our BO algorithm with $\lambda = 0$.
- 4) **Explore-only:** selects the object orientation and section with the most uncertainty. This is equivalent to our BO algorithm with $\lambda \rightarrow \infty$.

The maximum exploration time allowed is 10 steps.

Quantitative results. Each result is evaluated over 15 objects with 72 initial grasping points. All methods are able to perform with a high success rate given enough exploration steps $> 98\%$. However, our BO-based exploration strategy consistently requires fewer exploration steps (Fig. 9). Over the randomly-generated set of objects, our BO approach performs better than exploit-only ($p < 0.001$), explore-only ($p < 0.01$), and the random baseline ($p < 0.001$). All p-values were computed using the paired-samples t-test.

B. Sensitivity analysis for noise

Noise in the reconstructed model. Noisy depth images and a noisy prior estimate on the object’s motion due to slipping could cause poor object reconstruction results. To evaluate the tolerance to poor object reconstruction, we add i.i.d. zero-mean Gaussian noise to the reconstructed point cloud before fitting the GP model. As shown in Fig. 10 (left), while the success rate deteriorates in all methods as noise increases, our method outperforms others in the low-to-medium noise regimes. For high-noise regime our method performs similarly to the exploit-only baseline.

Noise in the depth image. To evaluate the tolerance to noisy depth images, we add i.i.d. zero-mean Gaussian noise to the simulated depth images used for ICP reconstruction. Unlike adding noise to the reconstructed model, adding noise to depth images makes it harder for ICP to reconstruct the object model. Fig. 10 (right) demonstrates that while adding noise to the depth images affects the performance of all methods, our method has significant advantage in the low-to-medium noise regimes. When the standard deviation of the noise is smaller than 4 mm, our method can still reach a success rate above 80%. Higher noise levels can lead to a noticeable performance drop.

C. Real-world shape reconstruction

Given the scale of the tactile sensors on the Roller Grasper hardware, we 3D printed custom objects with heterogeneous

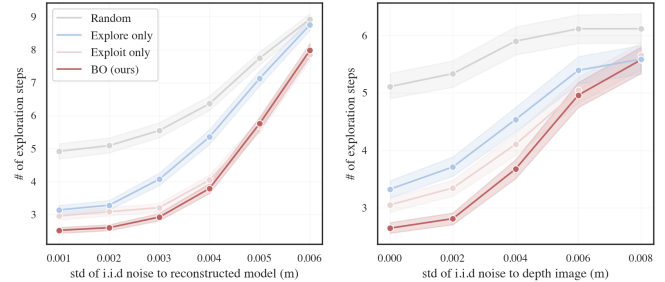


Fig. 10: Steps to finish the exploration with i.i.d. noise. Each bar is evaluated over 5 objects with 72 different initial grasping points.

surface textures in the form of random alphanumeric characters, as shown in Fig. 11(a). Fig. 11(b) shows qualitative results for the reconstruction of the global object shape after three exploration steps with these objects using the Roller Grasper hardware. This reconstruction leverages the measured kinematics as the Roller Grasper manipulates the object, refined using ICP between local pairs of depth maps as described in Section III-A.

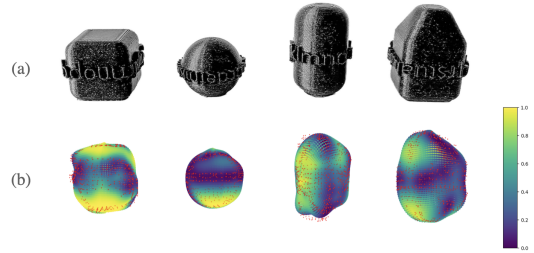


Fig. 11: Top: Four real objects manipulated by the Roller Grasper hardware. Bottom: Gaussian reconstruction of the object shape. Red points correspond to a down-sampled subset of the data collected by the tactile sensors.

V. CONCLUSION

In summary, we present a method to reorient unknown objects with tactile sensing that does not rely on vision. We perform in-hand simultaneous 3D shape reconstruction and localization, and outline an efficient strategy based on Bayesian optimization to select regions of the object to explore to ensure quick task completion. We demonstrated the efficacy of this method on the insertion task, suggesting its possible broad utility in tactile manipulation. For example, our approach could be applied to assembly tasks of small objects, and reorientation of objects in cluttered spaces.

For success on the currently available hardware, our work relies on several assumptions. Because we rely on local tactile data, our approach requires objects to have heterogeneous surface features in order to localize the robot on the object and align neighboring tactile depth maps. The hardware limitations of the Roller Grasper cause the need for object shapes to have aspect ratios close to 1. In future work, this limitation could be overcome by allowing regrasping. An additional complication is that objects may slip and drop in the early stages of exploration when the robot has very little object shape data. This limitation could be addressed via multimodal fusion with vision, which is a promising avenue for future work.

REFERENCES

- [1] OpenAI: Marcin Andrychowicz, Bowen Baker, Maciek Chociej, Rafal Jozefowicz, Bob McGrew, Jakob Pachocki, Arthur Petron, Matthias Plappert, Glenn Powell, Alex Ray, et al. Learning dexterous in-hand manipulation. *The International Journal of Robotics Research*, 39(1):3–20, 2020.
- [2] Nikhil Chavan-Dafle, Rachel Holladay, and Alberto Rodriguez. In-hand manipulation via motion cones. *arXiv preprint arXiv:1810.00219*, 2018.
- [3] Hanna Yousef, Mehdi Boukallel, and Kaspar Althoefer. Tactile sensing for dexterous in-hand manipulation in robotics—a review. *Sensors and Actuators A: physical*, 167(2):171–187, 2011.
- [4] Shenli Yuan, Lin Shao, Connor L Yako, Alex Gruebele, and J Kenneth Salisbury. Design and control of roller grasper v2 for in-hand manipulation. In *2020 IEEE/RSJ International Conference on Intelligent Robots and Systems (IROS)*, pages 9151–9158. IEEE, 2020.
- [5] Silvia Cruciani, Balakumar Sundaralingam, Kaiyu Hang, Vikash Kumar, Tucker Hermans, and Danica Kragic. Benchmarking in-hand manipulation. *IEEE Robotics and Automation Letters*, 5(2):588–595, 2020.
- [6] Andrew S. Morgan, Kaiyu Hang, Bowen Wen, Kostas Bekris, and Aaron M. Dollar. Complex in-hand manipulation via compliance-enabled finger gaing and multi-modal planning. *IEEE Robotics and Automation Letters*, 7(2):4821–4828, 2022.
- [7] Aditya Bhatt, Adrian Sieler, Steffen Puhlmann, and Oliver Brock. Surprisingly robust in-hand manipulation: An empirical study. *arXiv preprint arXiv:2201.11503*, 2022.
- [8] Tao Chen, Jie Xu, and Pulkit Agrawal. A system for general in-hand object re-orientation. In *Conference on Robot Learning*, pages 297–307. PMLR, 2022.
- [9] Pietro Falco, Shuang Lu, Andrea Cirillo, Ciro Natale, Salvatore Pirozzi, and Dongheui Lee. Cross-modal visuo-tactile object recognition using robotic active exploration. In *2017 IEEE International Conference on Robotics and Automation (ICRA)*, pages 5273–5280, 2017.
- [10] Sudharshan Suresh, Zilin Si, Joshua G Mangelson, Wenzhen Yuan, and Michael Kaess. Shapemap 3-d: Efficient shape mapping through dense touch and vision. In *2022 International Conference on Robotics and Automation (ICRA)*, pages 7073–7080. IEEE, 2022.
- [11] Edward Smith, Roberto Calandra, Adriana Romero, Georgia Gkioxari, David Meger, Jitendra Malik, and Michal Drozdal. 3d shape reconstruction from vision and touch. *Advances in Neural Information Processing Systems*, 33:14193–14206, 2020.
- [12] Monika A Schaeffer and Allison M Okamura. Methods for intelligent localization and mapping during haptic exploration. In *SMC'03 Conference Proceedings. 2003 IEEE International Conference on Systems, Man and Cybernetics. Conference Theme-System Security and Assurance (Cat. No. 03CH37483)*, volume 4, pages 3438–3445. IEEE, 2003.
- [13] Anna Petrovskaya and Oussama Khatib. Global localization of objects via touch. *IEEE Transactions on Robotics*, 27(3):569–585, 2011.
- [14] Danny Driess, Peter Englert, and Marc Toussaint. Active learning with query paths for tactile object shape exploration. In *2017 IEEE/RSJ International Conference on Intelligent Robots and Systems (IROS)*, pages 65–72. IEEE, 2017.
- [15] Rui Li, Robert Platt, Wenzhen Yuan, Andreas ten Pas, Nathan Roscup, Mandayam A Srinivasan, and Edward Adelson. Localization and manipulation of small parts using gelsight tactile sensing. In *2014 IEEE/RSJ International Conference on Intelligent Robots and Systems*, pages 3988–3993. IEEE, 2014.
- [16] Maria Bauza, Oleguer Canal, and Alberto Rodriguez. Tactile mapping and localization from high-resolution tactile imprints. In *2019 International Conference on Robotics and Automation (ICRA)*, pages 3811–3817. IEEE, 2019.
- [17] Maria Bauza, Eric Valls, Bryan Lim, Theo Sechopoulos, and Alberto Rodriguez. Tactile object pose estimation from the first touch with geometric contact rendering. *arXiv preprint arXiv:2012.05205*, 2020.
- [18] Shan Luo, Wenxuan Mou, Kaspar Althoefer, and Hongbin Liu. Localizing the object contact through matching tactile features with visual map. In *2015 IEEE International Conference on Robotics and Automation (ICRA)*, pages 3903–3908, 2015.
- [19] Yu She, Shaoxiong Wang, Siyuan Dong, Neha Sunil, Alberto Rodriguez, and Edward Adelson. Cable manipulation with a tactile-reactive gripper. *The International Journal of Robotics Research*, 40(12-14):1385–1401, 2021.
- [20] Sudharshan Suresh, Maria Bauza, Kuan-Ting Yu, Joshua G Mangelson, Alberto Rodriguez, and Michael Kaess. Tactile slam: Real-time inference of shape and pose from planar pushing. In *2021 IEEE International Conference on Robotics and Automation (ICRA)*, pages 11322–11328. IEEE, 2021.
- [21] Stanimir Dragiev, Marc Toussaint, and Michael Gienger. Gaussian process implicit surfaces for shape estimation and grasping. In *2011 IEEE International Conference on Robotics and Automation*, pages 2845–2850, 2011.
- [22] Marten Björkman, Yasemin Bekiroglu, Virgile Högman, and Danica Kragic. Enhancing visual perception of shape through tactile glances. In *2013 IEEE/RSJ International Conference on Intelligent Robots and Systems*, pages 3180–3186. IEEE, 2013.
- [23] Stanimir Dragiev, Marc Toussaint, and Michael Gienger. Uncertainty aware grasping and tactile exploration. In *2013 IEEE International conference on robotics and automation*, pages 113–119. IEEE, 2013.
- [24] Herman Bruyninckx, Stefan Dutre, and Joris De Schutter. Peg-on-hole: a model based solution to peg and hole alignment. In *Proceedings of 1995 IEEE International Conference on Robotics and Automation*, volume 2, pages 1919–1924. IEEE, 1995.
- [25] Siddharth R Chhatpar and Michael S Branicky. Search strategies for peg-in-hole assemblies with position uncertainty. In *Proceedings 2001 IEEE/RSJ International Conference on Intelligent Robots and Systems. Expanding the Societal Role of Robotics in the Next Millennium (Cat. No. 01CH37180)*, volume 3, pages 1465–1470. IEEE, 2001.
- [26] Hyeonjun Park, Jaeheung Park, Dong-Hyuk Lee, Jae-Han Park, Moon-Hong Baeg, and Ji-Hun Bae. Compliance-based robotic peg-in-hole assembly strategy without force feedback. *IEEE Transactions on Industrial Electronics*, 64(8):6299–6309, 2017.
- [27] Karl Van Wyk, Mark Culleton, Joe Falco, and Kevin Kelly. Comparative peg-in-hole testing of a force-based manipulation controlled robotic hand. *IEEE Transactions on Robotics*, 34(2):542–549, 2018.
- [28] Hee-Chan Song, Young-Loul Kim, and Jae-Bok Song. Automated guidance of peg-in-hole assembly tasks for complex-shaped parts. In *2014 IEEE/RSJ International Conference on Intelligent Robots and Systems*, pages 4517–4522, 2014.
- [29] Te Tang, Hsien-Chung Lin, Yu Zhao, Yongxiang Fan, Wenjie Chen, and Masayoshi Tomizuka. Teach industrial robots peg-hole-insertion by human demonstration. In *2016 IEEE International Conference on Advanced Intelligent Mechatronics (AIM)*, pages 488–494, 2016.
- [30] Michelle A. Lee, Yuke Zhu, Krishnan Srinivasan, Parth Shah, Silvio Savarese, Li Fei-Fei, Animesh Garg, and Jeannette Bohg. Making sense of vision and touch: Self-supervised learning of multimodal representations for contact-rich tasks. In *2019 International Conference on Robotics and Automation (ICRA)*, pages 8943–8950, 2019.
- [31] Shenli Yuan. *Robot in-hand manipulation using Roller Graspers*. PhD thesis, Stanford University, 2022.
- [32] Wenzhen Yuan, Siyuan Dong, and Edward H Adelson. Gelsight: High-resolution robot tactile sensors for estimating geometry and force. *Sensors*, 17(12):2762, 2017.
- [33] Szymon Rusinkiewicz and Marc Levoy. Efficient variants of the icp algorithm. In *Proceedings third international conference on 3-D digital imaging and modeling*, pages 145–152. IEEE, 2001.
- [34] Sungjoon Choi, Qian-Yi Zhou, and Vladlen Koltun. Robust reconstruction of indoor scenes. In *Proceedings of the IEEE Conference on Computer Vision and Pattern Recognition*, pages 5556–5565, 2015.
- [35] Donald R Jones, Matthias Schonlau, and William J Welch. Efficient global optimization of expensive black-box functions. *Journal of Global optimization*, 13(4):455–492, 1998.
- [36] Bobak Shahriari, Kevin Swersky, Ziyu Wang, Ryan P Adams, and Nando de Freitas. Taking the Human Out of the Loop: A Review of Bayesian Optimization. *Proceedings of the IEEE*, 104(1):148–175, 2016.
- [37] Christopher KI Williams and Carl Edward Rasmussen. *Gaussian processes for machine learning*, volume 2. MIT press Cambridge, MA, 2006.
- [38] Niranjan Srinivas, Andreas Krause, Sham Kakade, and Matthias Seeger. Gaussian process optimization in the bandit setting: No regret and experimental design. pages 1015–1022, 07 2010.
- [39] Erwin Coumans and Yunfei Bai. Pybullet, a python module for physics simulation for games, robotics and machine learning. <http://pybullet.org>, 2016–2021.